

The applicability of the Chemical Index of Alteration as a paleoclimatic indicator: An example from the Permian of the Paraná Basin, Brazil

Karin Goldberg^{a,*}, Munir Humayun^b

^a Universidade Federal do Rio Grande do Sul (UFRGS), Programa de Geologia do Petróleo, Av. Bento Gonçalves, 9500 Prédio 43137 Sala 203 Porto Alegre, RS 91509-900, Brazil

^b Florida State University, National High Magnetic Field Laboratory & Department of Geological Sciences, 1800 E. Paul Dirac Drive, Tallahassee, FL 32310, USA

ARTICLE INFO

Article history:

Received 22 May 2009

Received in revised form 27 April 2010

Accepted 25 May 2010

Available online 1 June 2010

Keywords:

Paleoclimatology

Weathering

Permian

Paraná Basin

Chemical index of alteration

ABSTRACT

The Chemical Index of Alteration (CIA) was expressed as CIA (molar) to become a more sensitive measure of the degree of chemical weathering. The CIA (molar) has the value of 1 for fresh feldspars and for unweathered, non-peraluminous igneous rocks, but increases towards infinity as chemical weathering progresses. The utility of this index as a humidity indicator for both modern and ancient muds was tested. A database comprising 281 entries with chemical data for modern and ancient sediments deposited under arid, semi-arid, semi-humid and humid climate was assembled from the literature, and used to calibrate the relationship between humidity and CIA (molar) values. For both modern and ancient sediments, the histograms display a shift towards higher values with increasing geological indicators of humidity, whereas sediments deposited under conditions inferred to be arid from other geological indicators show values tightly clustered around 1. The Permian of the Paraná Basin was then used as an example of the applicability of the CIA (molar) for paleoclimatic studies. Major element analyses (Al_2O_3 , K_2O , Na_2O , CaO) were performed on 55 claystones and shales from three drill cores in a stratigraphic succession spanning the Early to Late Permian. The CIA (molar) for these rocks accorded with expectations based on sedimentologic and paleontologic evidence, discriminating well between arid and humid conditions in the basin independently determined from sedimentological and paleontological indicators. The use of the CIA (molar) as a paleo-humidity indicator, however, can be limited by the presence of carbonate-rich sediments, the occurrence of post-depositional K^+ addition (metasomatism, metamorphism, diagenetic illitization), as well as by inheritance of clays from sedimentary rocks in the source area. Nevertheless, with appropriate caution, the CIA (molar) is a useful tool for the assessment of the humidity conditions in the rock record.

© 2010 Elsevier B.V. All rights reserved.

1. Introduction

The Chemical Index of Alteration (CIA) was proposed by Nesbitt and Young (1982) as a measure of the role played by chemical weathering in the production of clastic sediments. The ratio $\text{CIA} = (\text{Al}_2\text{O}_3/\text{Al}_2\text{O}_3 + \text{CaO}^* + \text{Na}_2\text{O} + \text{K}_2\text{O}) \times 100$ (where CaO^* is the calcium content of silicates) is based on the assumption that the dominant process during chemical weathering is the degradation of feldspars and the formation of clay minerals.

The importance of chemical weathering increases proportionately under humid conditions, with leaching of the alkalis (Na^+ , K^+) and Ca^{+2} , and concentration of Al and Si in the residue. Conversely, in an environment dominated by physical weathering, abrasion is the primary producer of sediments by mechanical breakdown into smaller grain sizes. The chemical alteration of feldspars to form clay minerals is thus negligible under physical weathering.

The CIA values for average shales range from 70 to 75 (Nesbitt and Young, 1982). The large amount of aluminous clay minerals (such as kaolinite) formed during intensive chemical weathering is reflected in the high CIA values (80–100) of muds formed under tropical conditions. On the other hand, in glacial environments, where abrasion is dominant over chemical weathering, common CIA values range from 50 to 70 (Nesbitt and Young, 1982).

The use of the CIA in paleoclimatic studies assumes that this index is a measurement of the amount of the chemical weathering undergone by the studied rocks. However, there are other factors that may affect the CIA and need to be taken into account, including sediment provenance, hydraulic sorting, and post-depositional processes that lead to K^+ addition (e.g. diagenetic illitization and metasomatism).

The contribution of different source rocks to the formation of sediments can be examined by the use of the A–CN–K plot (Nesbitt and Young, 1984, 1989; Akarish and El-Gohary, 2008) and/or the Ti/Al ratio (Maynard, 1992; Sheldon, 2006; Sheldon and Tabor, 2009).

Hydraulic sorting can significantly influence the chemical composition of terrigenous sediments due to grain size and mineral sorting (Bauluz et al., 2000). For instance, aluminum is concentrated in the

* Corresponding author. Fax: +55 51 3308 7047.

E-mail address: karin.goldberg@ufrgs.br (K. Goldberg).

clays, hence the larger the transport (i.e. distal regions), the finer the sediments and the higher the Al concentration (Soreghan and Soreghan, 2007). There is also a tendency of larger grain sizes to concentrate feldspars, which leads to lower CIA values (Visser and Young, 1990; Zimmerman and Bahlburg, 2003).

Several authors have observed the need to correct for later K^+ addition due to processes such as illitization and metasomatism (e.g. Maynard, 1992; Fedo et al., 1995; Price and Velbel, 2003). The calculation of $CIA-K = 100 \times (Al_2O_3/Al_2O_3 + CaO + Na_2O)$ (Maynard,

1992) was an attempt to avoid this problem. Fedo et al. (1995) suggested that the extent of metasomatic processes that have affected a particular sandstone can be determined petrographically and the original CIA value prior to K enrichment can be determined through the use of A–CN–K compositional space to constrain the initial composition of source rocks.

The CIA designed by Nesbitt and Young (1982) is calculated on the basis of major element chemistry of lutites. This method has been largely applied to the study of weathering trends in ancient mudstones

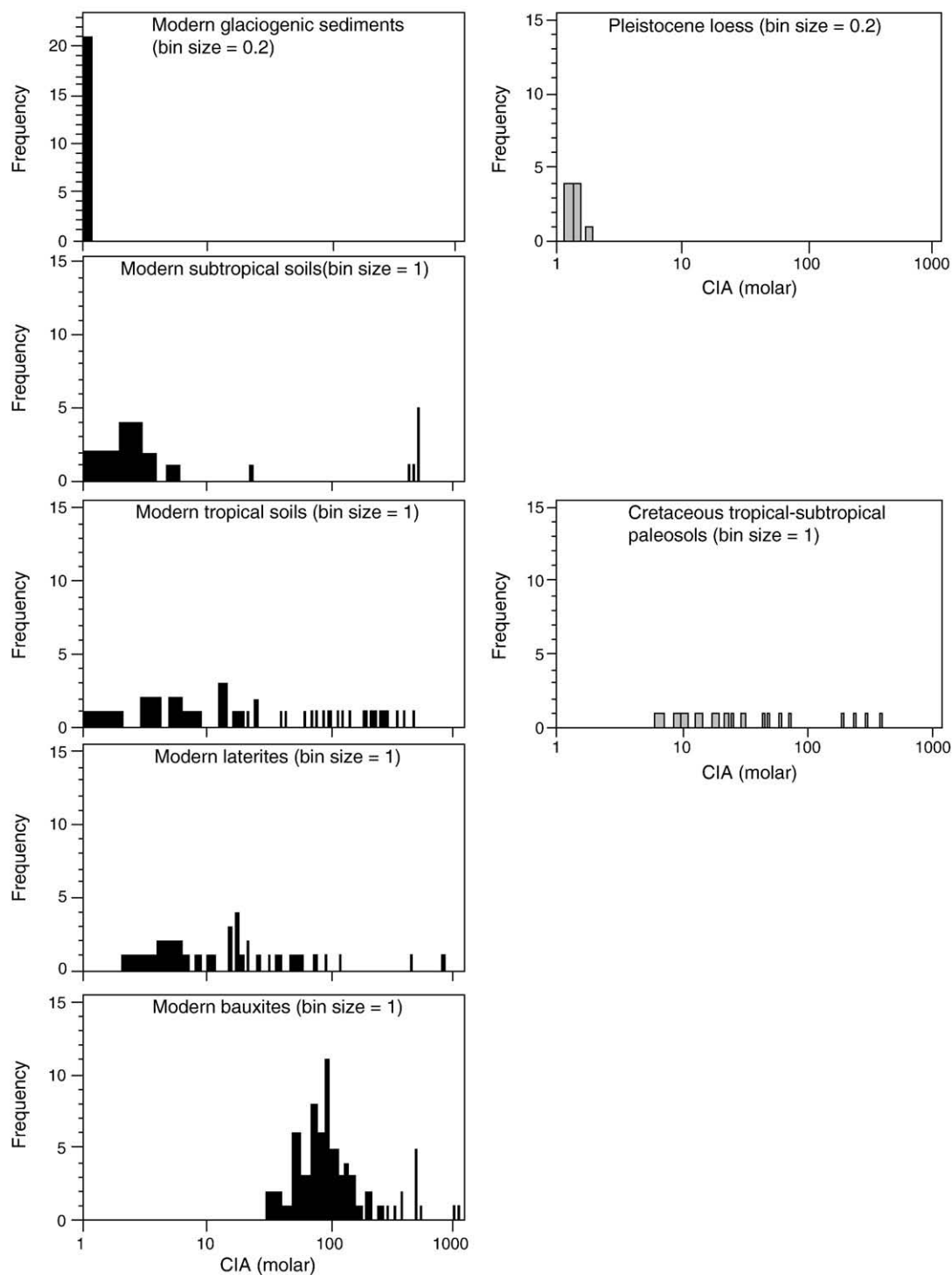


Fig. 1. Frequency histograms of CIA (molar) values for muds and soils deposited under different precipitation conditions (increasing precipitation balance from top to bottom). Data on modern sediments shown on the left column (histograms in black) and on ancient environments on the right (histograms in gray). Note the log scale on the x-axis. The bins refer to the subdivision in the histograms, and the bin size is the number of CIA (molar) units per bar.

(e.g. Visser and Young, 1990; Young et al., 1998; Young and Nesbitt, 1999; Young, 2002; Rashid, 2005; Alvarez and Roser, 2007; Sinha et al., 2007; Kasanzu et al., 2008; Zaghoul et al., 2010), as well as for the study of paleosols (e.g. Sheldon, 2003, 2005; Driese et al., 2005; Sheldon, 2006; Sayyed and Hundekari, 2006; Zech et al., 2008; Singh et al., 2009).

The wide application of the CIA index has led to some improper use of the method originally proposed. The literature provides examples of the application of the CIA for variable grain sizes (comparing sandstones and mudstones, for instance), including the calcium content in carbonates (rather than only in the silicate fraction), and ignoring clear post-depositional additions of K^+ (e.g. Bauluz et al., 2000; Gu et al., 2002; Perez-Huerta and Sheldon, 2006; Minyuk et al.,

2007; Rahman and Suzuki, 2007; Akarish and El-Gohary, 2008; Spalletti et al., 2008; Gallala et al., 2009), all factors which may render the results unreliable.

Nonetheless, the utility of the CIA in paleoclimatic studies has already been ascertained, and some studies have gone as far as establishing and testing the relation between the CIA and mean annual precipitation and temperature (Sheldon et al., 2002; Retallack, 2005, 2009; Hamer et al., 2007a,b).

In this study, we examine the CIA (molar) to attain a more sensitive measure of the degree of chemical weathering, demonstrating its utility as a humidity indicator for both modern and ancient muds. We present chemical analyses of 55 mudrock samples from a

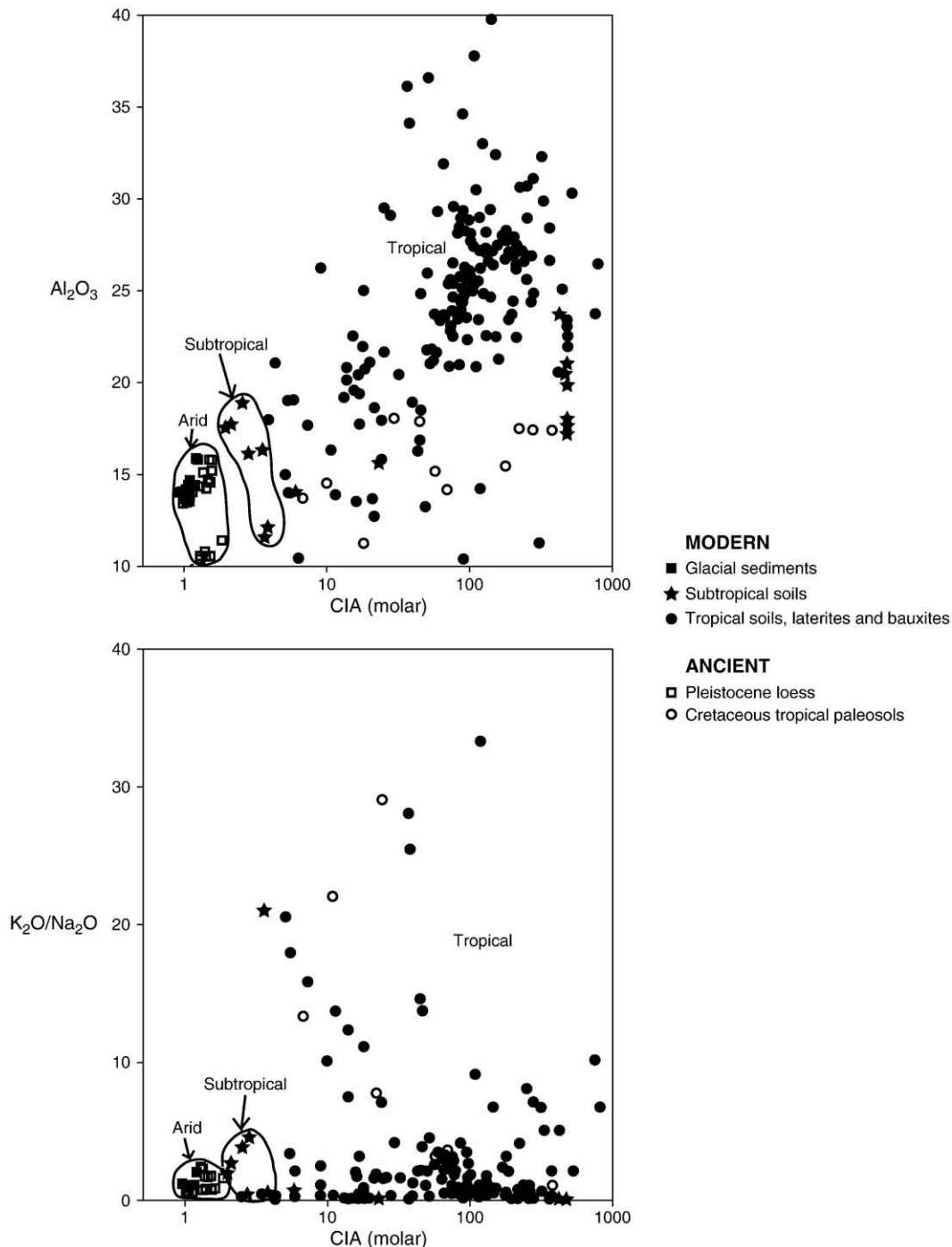


Fig. 2. Scatter plot of CIA (molar) versus Al_2O_3 (top) and K_2O/Na_2O (bottom). Squares are glacial sediments, diamonds are subtropical, and circles are tropical sediments. Solid symbols are data on modern muds and open symbols on ancient ones.

stratigraphic section of Early to Late Permian from the Paraná Basin and apply the CIA (molar) as a weathering index for paleoclimatic studies in samples for which sedimentological and paleontological constraints are also available (Goldberg, 2001).

2. The Chemical Index of Alteration (molar)

The Chemical Index of Alteration (CIA), as defined by Nesbitt and Young (1982), has a limited range of variability due to the constraint imposed by summing to 100%. We used the convention of converting the raw abundances into moles by dividing the weight percent by molecular weight, which gives the relative abundance on an atomic stoichiometric basis (Retallack, 1997, 2001; Sheldon and Tabor, 2009). In this way, the CIA (molar) results in a proportion between alumina and alkalis plus calcium $[CIA_{\text{molar}} = Al_2O_3(\text{molar}) / (CaO^*_{\text{molar}} + Na_2O_{\text{molar}} + K_2O_{\text{molar}})]$, becoming a more sensitive measure of the degree of chemical weathering.

The advantage of using the molar ratio in the calculation of the index is that CIA (molar) values are easily translated into degree of chemical weathering when compared with the proportion between Al, alkalis and Ca in the chemical formula of known minerals. For example, the molar ratio of K and Na to Al in alkali feldspars $[(K,Na)AlSi_3O_8]$ is 1:1. For illite $[K_{1.5-1.0}Al_4[Si_{6.5-7.0}Al_{1.5-1.0}O_{20}](OH)_4]$, the molar ratio of K to Al is 1:4. Hence, the CIA (molar) index of fresh feldspars (and for unweathered, non-peraluminous igneous rocks) is 1, but rises towards infinity as chemical weathering progresses. With increasing chemical alteration, CIA (molar) values increase due to the alteration of feldspars to clay minerals, reaching the illite value of 4. Further chemical weathering produces laterites and bauxites, which display greater CIA (molar) values. CIA (molar) values smaller than 1 for clastic sediments may indicate the presence of carbonates, which must be removed by leaching the sediments with acetic acid prior to chemical analysis.

Therefore, the CIA (molar) index can be used to define the degree of chemical weathering (and thus humidity fields) of clastic sediments, provided it is calibrated against the composition of modern sediments deposited under known weathering conditions. The CIA (molar) ratio has been used to obtain paleo-precipitation from Permian sediments (Retallack, 2009).

3. The CIA (molar) as an indicator of chemical weathering in modern sediments

A database comprising 281 entries with chemical data for modern and ancient sediments deposited under arid, semi-arid, semi-humid and humid climate was assembled from the literature, and used to calibrate the relationship between humidity and CIA (molar) values. A summary of the database is available upon request to the corresponding author.

The compilation of the database took into account the following criteria: i) data on the concentrations of Al_2O_3 , K_2O , Na_2O and CaO in muds and soils were collected only for regions where the climatic setting was clearly stated by the authors; ii) all the carbonate-bearing sediments were excluded, since the CaO concentration reported in the literature included the calcium content of both silicate and carbonate fractions, not appropriate for CIA calculations; iii) sediments affected by metasomatism or metamorphism were also excluded, as later additions of K^+ might have occurred; iv) the sum of alkalis necessarily had to be greater than zero, since it is the denominator in the calculation of the CIA (molar); and v) the oxide concentration was entered as “zero” when reported to be less than 0.01 wt.%.

The data are shown in Fig. 1. The histograms display a shift towards higher values with increasing geological indicators of humidity, whereas sediments deposited under conditions inferred to be arid from other geological indicators show values tightly clustered around 1. The CIA (molar) values for both modern and Pleistocene arid environments are close to 1 (denoting the presence of pristine feldspars), whereas they are progressively more scattered and higher toward tropical sediments for both modern and Cretaceous soils. As

expected, the most extreme values are found in laterites and bauxites, with values greater than 1000. The histogram for modern subtropical soils displays a small group of samples with CIA (molar) values much higher than the mode. These values correspond to a study carried out in subtropical soils collected in southern Brazil (Melfi et al., 1983), and the spurious results are due to the reported K_2O concentration being zero for this specific group of samples, and should perhaps be excluded from the climate group. Then, modern subtropical soils (with one exception) have CIA (molar) < 10 .

A similar trend can be observed if the data is displayed on XY diagrams (Fig. 2). Once again, CIA (molar) values for sediments from arid settings cluster around 1, whereas muds deposited under tropical conditions lie consistently above the illite CIA (molar) value of 4. Hence the CIA (molar) of both modern and ancient sediments

Table 1

Chemical analysis (in weight percent) and CIA (molar) data for mudrocks from the Permian of the Paraná Basin.

Core	Sample	Strat. unit	Na ₂ O	CaO	K ₂ O	Al ₂ O ₃	CIA (molar)
CA-53	48	Sanga do Cabral Fm.	1.12	0.24	3.87	17.4	2.69
	125.7	Sanga do Cabral Fm.	0.99	0.17	4.43	18.3	2.72
	164	Rio do Rasto Fm.	1.36	0.32	4.89	18.4	2.26
	202	Teresina Fm.	0.36	0.61	1.13	5.2	1.78
	220.4	Teresina Fm.	1.12	1.49	2.80	15.4	2.04
	240.1	Teresina Fm.	1.97	1.17	2.85	10.4	1.23
	257.7	Serra Alta Fm.	1.52	1.05	3.69	17.8	2.12
	271.4	Serra Alta Fm.	1.28	0.44	3.59	17.0	2.51
	298.6	Irati Fm.	2.53	1.22	2.72	15.7	1.69
	325.7	Palermo Fm.	1.60	0.31	3.16	15.9	2.42
	350.4	Palermo Fm.	2.33	0.65	3.56	18.3	2.07
	364	R. Bonito/Palermo	1.79	0.13	2.54	17.6	2.97
	389.1	R. Bonito/Palermo	1.24	0.067	2.77	21.5	4.17
	412.4	Rio Bonito Fm.	0.087	0.029	1.23	24.5	16.03
	432	Rio Bonito Fm.	0.71	1.40	3.83	19.0	2.43
	438.8	Rio Bonito Fm.	0.24	0.018	1.93	24.5	9.78
	470.8	Rio Bonito Fm.	0.72	0.029	2.49	26.0	6.61
	529.1	Itararé Gr.	3.55	0.43	4.63	17.2	1.48
	547.2	Itararé Gr.	3.05	0.26	5.14	12.2	1.1
	555	Itararé Gr.	3.52	1.70	4.30	13.5	1
	561	Itararé Gr.	4.05	0.30	4.32	12.3	1.03
	580.2	Itararé Gr.	2.28	0.22	3.29	11.6	1.5
CA-79	198.2	Sanga do Cabral Fm.	1.49	0.61	5.02	18.1	2.01
	262.3	Sanga do Cabral Fm.	2.02	0.94	4.79	15.0	1.47
	357.8	Morro Pelado Mb.	1.99	0.40	6.22	17.4	1.63
	409.4	Morro Pelado Mb.	2.06	0.63	5.29	15.4	1.5
	456.5	Morro Pelado Mb.	2.32	0.95	5.28	14.8	1.31
	501.4	Morro Pelado Mb.	2.12	0.60	5.96	18.7	1.69
	523.8	Serrinha Mb.	4.25	1.91	1.52	14.4	1.19
	534.4	Serrinha Mb.	6.52	0.52	2.79	22.0	1.5
	588.4	Serrinha Mb.	5.86	0.45	1.57	11.1	0.92
	614.1	Teresina Fm.	1.63	0.85	4.65	18.0	1.94
	649.8	Serra Alta Fm.	1.75	1.43	3.59	16.4	1.75
	671.4	Serra Alta Fm.	1.22	0.43	2.49	12.7	2.31
	681.4	Irati Fm.	1.18	0.36	3.10	14.0	2.35
	698.3	Irati Fm.	1.57	0.99	2.83	15.9	2.14
	723.6	Irati Fm.	1.18	0.53	3.61	15.1	2.23
	747.2	Palermo Fm.	2.10	0.70	3.22	16.2	1.98
	769.7	Palermo Fm.	1.80	0.94	2.79	17.9	2.33
	802.5	R. Bonito/Palermo	1.13	0.18	3.51	19.1	3.2
	818.9	R. Bonito/Palermo	0.80	0.29	2.56	22.0	4.77
	845.5	Rio Bonito Fm.	0.57	0.12	1.91	19.0	5.89
CA-87	868.9	Rio Bonito Fm.	0.16	0.03	1.50	24.1	12.54
	883	Rio Bonito Fm.	0.92	0.04	2.46	21.7	5.09
	886.6	Rio Bonito Fm.	1.00	0.33	1.80	12.2	2.89
	132	Botucatu Fm.	1.10	1.57	3.89	15.7	1.77
	185.5	Sanga do Cabral Fm.	2.16	0.77	8.02	31.3	2.3
	240.8	Sanga do Cabral Fm.	2.39	0.79	5.16	16.8	1.53
	282	Sanga do Cabral Fm.	1.96	1.36	5.77	15.1	1.27
	301.5	Sanga do Cabral Fm.	2.87	2.32	2.80	9.96	0.83
	378	Morro Pelado Mb.	2.18	1.25	4.97	12.6	1.12
	437.5	Serrinha Mb.	3.19	3.37	2.10	9.78	0.72
	520.2	Irati Fm.	2.55	2.31	2.64	21.0	1.87
	554.1	Irati Fm.	0.67	16.9	0.61	3.50	0.11
	580.5	Palermo Fm.	2.46	1.31	2.72	14.1	1.51

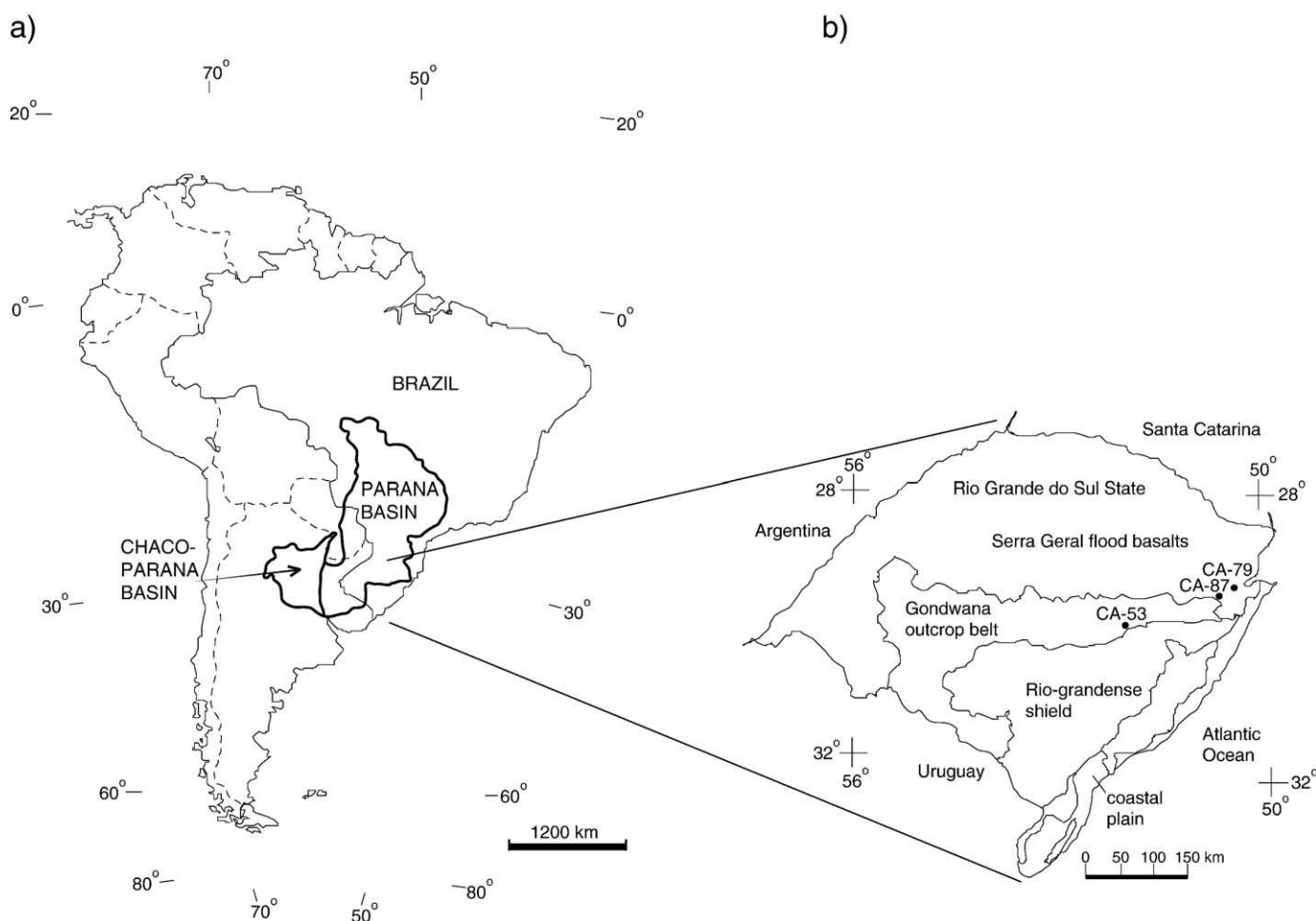


Fig. 3. Geographic localization of the Paraná and Chaco-Paraná Basins in South America (after Zálan et al., 1991), and the drill cores sampled for this study in southern Brazil.

deposited in settings with different conditions of humidity is quite distinctive, at least for the end-members, validating the use of this index a humidity indicator.

Although the CIA is a widely-used weathering index, Xiao et al. (2010) have warned of a potential problem with the application of the CIA regarding autocorrelation, which is the cross-correlation of a signal with itself. The CIA value of a sample may not reflect the exact climate conditions during the time of deposition because of its autocorrelation in sedimentary profiles, particularly for loess samples. Therefore, the application of this index must comprise a careful analysis of the succession investigated, preferably including other indicators of the climatic conditions, e.g. sedimentological and/or paleontological proxies.

4. Sample preparation and analytical techniques

The CIA (molar) method can be applied to mudrocks in general. However, in order to avoid possible effects due to hydraulic fractionation (as previously discussed), it is desirable that the elemental analysis for CIA (molar) calculations is carried out in: (a) samples with a limited range in grain size, either clay-sized (<0.004 mm) or silt-sized (between 0.004 and 0.0062 mm) rocks, (b) pristine samples, devoid of alteration due to recent/sub-recent weathering processes (in this regard, samples from drill cores are preferable to outcrop samples), and (c) siliciclastic mudrocks, with low carbonate content (<30% carbonate), and with removal of carbonate to ensure that the CaO measured is the calcium content in silicates. In the present study, any carbonate present was leached with 50% acetic acid prior to sample dissolution.

The samples selected for CIA (molar) analysis were hand-ground in agate mortars, ultrasonically cleaned, and approximately 200 mg powder was weighed into polypropylene centrifuge tubes, to which 50% acetic acid was added to remove carbonates. The acetic acid leachate was discarded and the siliciclastic residues were transferred to Savillex™ PFA vials, to which 3 ml of HF and 2 ml of HCl were then added for dissolution. The vials were then sealed and heated on a hot plate at 160 °C for 12 h in a Class 100 cleanroom. The contents were then opened and evaporated to dryness. The solid residue was taken up in 2 ml of HClO₄ and fumed to remove silica. After the perchloric acid dry-downs, the solids were re-dissolved in 6 ml of 8 N HNO₃, then sealed and heated on a hot plate for 12 h. The solutions were then centrifuged to remove any residue and transferred to Nalgene™ 125 ml LDPE bottles. To ensure complete dissolution of insoluble alkali perchlorates, the residual material was re-dissolved with 8 N HNO₃, and heated on a hot plate for 12 h. The solutions were subsequently diluted with 2% HNO₃ for analysis by Atomic Absorption Spectrophotometry.

Elemental concentrations of Al, Ca, K and Na were measured in a SpectrAA 220 atomic absorption spectrometer, using a nitrous oxide – acetylene flame for Ca and Al, and an air – acetylene flame for K and Na analyses. The wavelengths for each of the elements are as follows: 422.7 nm for Ca, 309.3 nm for Al, 766.5 nm for K, and 589.0 nm for Na. To suppress ionization in Na and K analyses, the samples were spiked with a Li nitrate solution to give a final concentration of 1 mg/ml. For Al analysis, the addition of a La nitrate solution (also 1 mg/ml) was necessary to minimize the effect of Si, Ca and phosphate on Al absorbance. Based on replicate analyses, the percent standard deviations were typically 5% for Al, 4% for Ca, and 2% for K and Na.

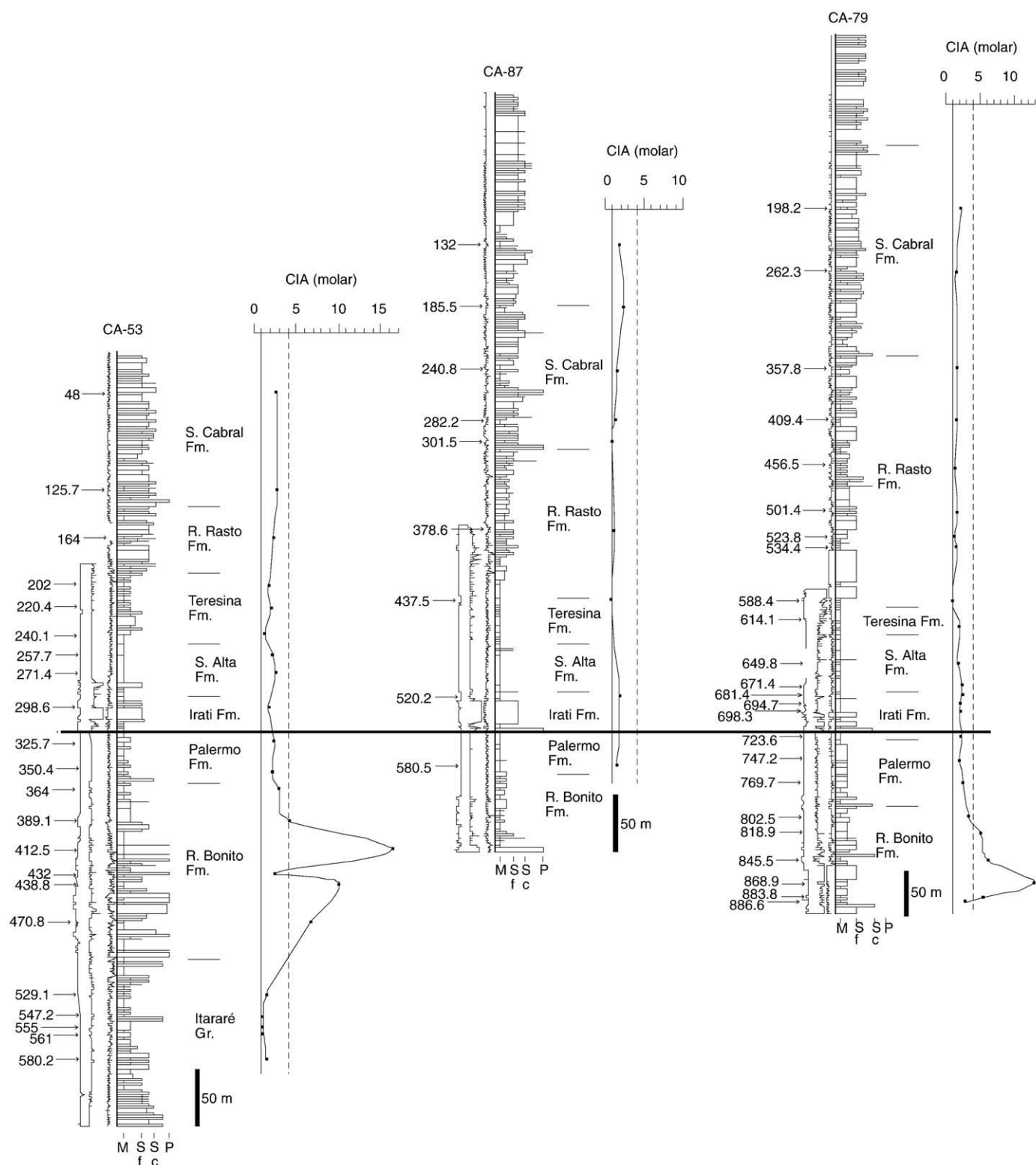


Fig. 4. CIA (molar) for the samples from cores CA-53, CA-87 and CA-79, plotted on their respective lithologic logs. The lines in CIA (molar) graphs represent feldspar (solid) and illite (dashed) lines. Abbreviations in the grain size scale are M (mud), Sf (fine sand), Sc (coarse sand) and P (pebble). The correlation datum is the base of the Irati Formation. Sample numbers refer to the depth (in meters) down core.

The measured elemental concentrations are reported as oxide abundances in Table 1. Table 1 also provides the CIA (molar) for the samples calculated according to the formula $CIA_{molar} = Al_2O_{3(molar)} / (CaO^*_{molar} + Na_2O_{molar} + K_2O_{molar})$, where CaO^* is the Ca-content of the silicate fraction of the sediment.

5. Application in the Permian of the Paraná Basin

The Permian units of the Paraná Basin (Fig. 3a) was used as an example of the applicability of the CIA (molar) to paleoclimatic studies because these rocks record an extreme climate change from

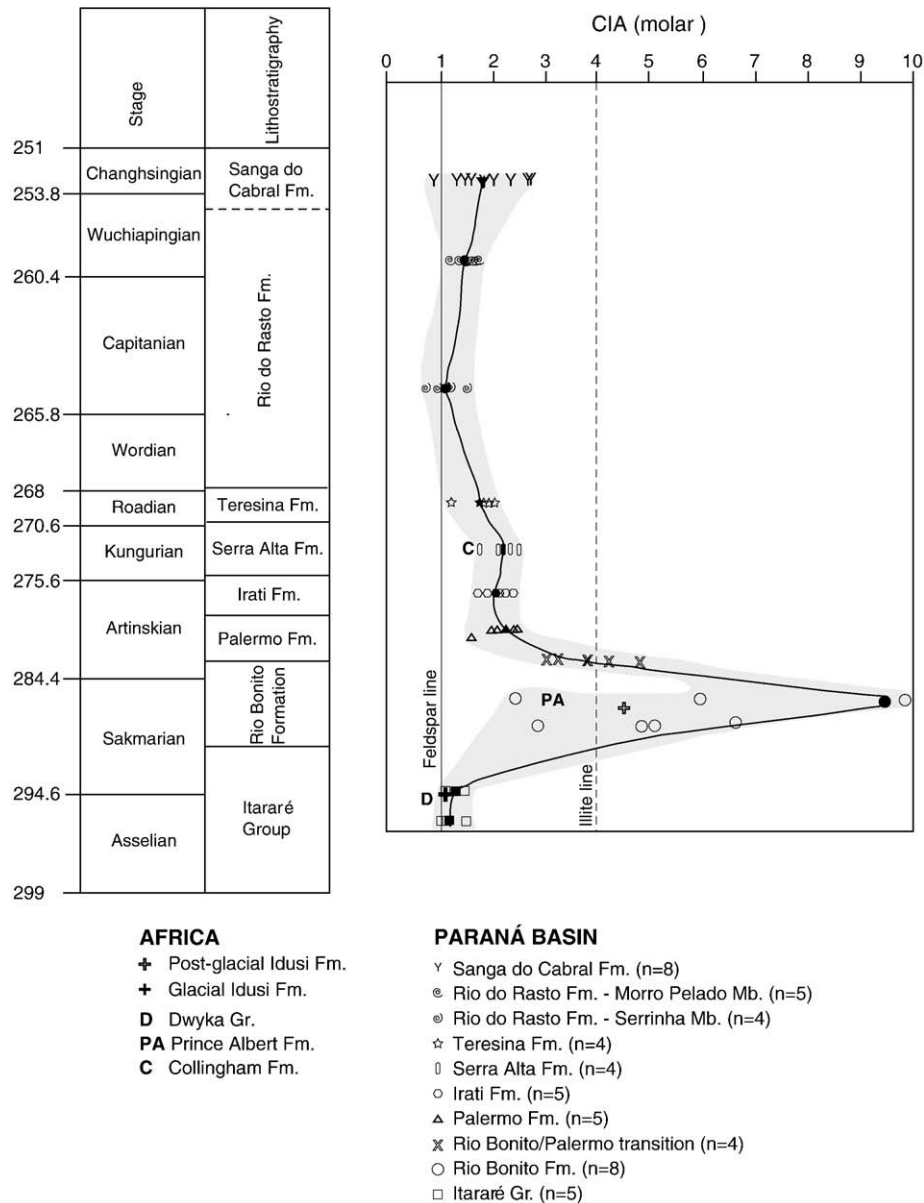


Fig. 5. CIA (molar) of the Permian units of the Paraná Basin, integrating data from cores CA-53, CA-79 and CA-87. The open symbols are individual data points, whereas the solid symbols are the average for their respective stratigraphic unit. One of the data points for the Rio Bonito Fm. falls off the graph [CIA (molar) = 16.03]. Chronostratigraphic framework from Santos et al. (2006). Data on the Idusi Formation from Diekmann and Wopfner (1996), and data on the Karoo Basin from Scheffler et al. (2003, 2006).

Early to Late Permian, well documented in other geological and paleontological archives (Gravenor and Rocha-Campos, 1983; Fairchild et al., 1985; Rohn and Fairchild, 1985; Lavina and Faccini, 1993; Nowatzki et al., 1996; Santos et al., 1996; Ziegler et al., 1997; Guerra-Sommer and Cazzulo-Klepzig, 2000; Goldberg, 2001). The Permian succession starts with the glacial deposits of the Itararé Group, overlain by the coal-bearing Rio Bonito Formation and the transgressive Palermo Formation. During maximum flooding of the basin, the Irati and Serra Alta Formation were deposited. Regression in the basin started with the deposition of the platform Teresina Formation, followed by the fluvial-lacustrine Rio do Rasto Formation and the eolian Sanga do Cabral Formation in the Late Permian. Hence, the expectation is that the CIA (molar) will reflect the change from arid cold (glacial) to humid (coal) and finally to arid (desertic).

Major element analysis (Al_2O_3 , K_2O , Na_2O , CaO) was performed for 55 claystones and shales from three wells drilled by the Brazilian Geological Survey in southern Brazil, CA-53, CA-79 and CA-87 (Table 1).

Locations of the drill cores are given in Fig. 3b. The sample numbers refer to the depth (in meters) down core.

The use of drill cores yielded the continuous recovery of the Permian section and the selection of pristine samples that have escaped modern tropical weathering. Twenty-two samples were collected from core CA-53, twenty-three from CA-79, and ten from CA-87. One sample from core CA-87 (554.1 m) was excluded due to its high carbonate content (45%).

These cores have sampled different stratigraphic sections of the Permian, thus the base of the Irati Formation was used as a datum for correlation between drill cores, to ascertain that equivalent stratigraphic sections were compared (Fig. 4). The base of the Irati Formation is a ubiquitous marker that can be identified both in the gamma-ray logs (as a radioactive peak) and in the lithologic logs (as carbonate breccias) (Goldberg, 2001).

The CIA (molar) calculated for the Permian sediments in the Paraná Basin yielded sensible results, discriminating well between arid and

humid conditions previously inferred from sedimentological or paleontological indicators. Here, we address the potential problems of diagenesis, illitization and potassium metasomatism in deeply buried rocks. Petrographic analysis of sandstones associated with the analyzed mudrocks indicates that illitization was minimum in the studied units. From the 52 thin sections analyzed (18 thin sections from CA-53, 16 thin sections from CA-79 and 18 thin sections from CA-87), only one thin section from CA-79 (at 795.6 m, corresponding to the Rio Bonito Formation) showed the presence of 2.5% illite. Diagenesis involving potassium addition is also insignificant, since only two thin sections from CA-53 (at depths of 624.9 and 630.8, corresponding to the Itararé Group) display 0.5 volume % of K-feldspar overgrowth. None of the analyzed thin sections has shown any signs of metasomatism, thus it is reasonable to assume that there was no significant K addition to create spurious results in the CIA calculations carried out in the Permian units of the Paraná Basin.

As shown in Fig. 4, the CIA (molar) for the analyzed cores displays the lowest values in the Itararé Group (plotting along the feldspar line), followed by a rapid increase to values above the illite line during the deposition of the coal-bearing Rio Bonito Formation. The drop in CIA (molar) values (to between the illite and the feldspar lines) observed in the middle portion of the Rio Bonito Formation seems to be associated with the presence of matrix-supported conglomerates, interpreted as debris-flow deposits. Above the Rio Bonito Formation, the CIA (molar) values oscillate between the illite and the feldspar lines, except for a pronounced drop in the upper Teresina – lower Rio do Rasto Formation.

The fluctuations of the CIA (molar) in the cores accords with expectation for the stratigraphic units, based on sedimentologic and paleontologic evidences. These variations can be translated in terms of changes in the degree of chemical weathering, where the low values of the Itararé Group, deposited under glacial influence, reflect an arid, abrasion-dominated environment. The high values of the Rio Bonito Formation, on the other hand, agree with a tropical or temperate, humid climate, in which high rainfall would favor the development of extensive vegetation, coal swamps and intense chemical weathering. The drop in CIA (molar) values at the upper Teresina Formation indicates an excursion to arid conditions. The existence of an arid setting in this unit is corroborated by the presence of gypsum veins, anhydrite and halite crystals associated with microbial lamination, which suggest that these sediments were deposited in a playa lake environment.

The CIA (molar) data points for the individual sequence stratigraphic units are displayed in Fig. 5 and listed in Table 1. Fig. 5 is a composite curve for the three cores from the Paraná Basin, on which CIA (molar) values of correlated Permian strata from Africa have been plotted. The same trends in the variation of the degree of chemical weathering observed in the individual cores emerge in the composite curve. Even though there is a substantial spread in the values, the paleoclimatic evolution outlined above appears once again, if the average values for each unit are taken into account.

It is interesting to observe that the CIA (molar) values calculated for correlated Permian stratigraphic units in Africa fall amidst the values for units in the Paraná Basin. The glacial sediments of the Idusi Formation (Diekmann and Wopfner, 1996) plot with the glacial Itararé Group, and the post-glacial deposits of the Idusi Formation plot with the Rio Bonito Formation. In the Karoo Basin (Scheffler et al., 2003, 2006), the calculated CIA (molar) for the Dwyka Group (correlative to the Itararé Group in the Paraná Basin), the Prince Albert Formation (Lower Ecca Group, correlative to the Rio Bonito Formation), and the Collingham Formation (Lower Ecca Group, correlative to the Serra Alta Formation), all plot close to the CIA (molar) values of their correlative units. The CIA study carried out by Scheffler et al. (2003, 2006) also showed a progressive decrease in CIA values in the Upper Ecca and Beaufort Groups, indicating decreasing chemical weathering and increasing aridity for the Permian units in the Karoo Basin. Thus, the African equivalents to the Permian of the Paraná in southern Brazil

provide corroboration of basin-wide paleoclimate variations in the Permian of Gondwanaland.

6. Conclusions

The chemical index of alteration, calculated as CIA (molar), seems to be a reasonable proxy for paleo-humidity, provided some limitations are taken into account:

- the CIA should not be used in carbonate-rich (>30% carbonate) sediments, and the samples should be treated with acetic acid prior to analysis to remove any carbonates present. A pre-treatment with acetic acid was proven efficient for this purpose, although dolomite is not as easily removed as calcite;
- sediments subjected to metasomatism, metamorphism or diagenetic illitization (the latter common in successions with interbedded evaporites) do not yield sensible CIA results, as they involve post-depositional additions of potassium. Hence it is essential to ascertain that the studied succession has not been subject to these processes;
- the CIA does not yield reliable results for samples submitted to recent/sub-recent alteration, as the original climatic signal may be overprinted;
- the most important restriction in the use of the molar CIA as a paleo-humidity indicator is the implicit assumption that the source area is composed predominantly by feldspathic igneous rocks, thus ignoring the effects of recycling of clastic sediments. In a basin where the source rocks are mostly sedimentary, the CIA of resulting mudrocks would bear a signature of chemical weathering cycles taking place at different moments, and very likely to be different from one another.

Nevertheless, with appropriate caution the CIA (molar) is a useful tool for the assessment of humidity conditions in the rock record, as demonstrated with the example from the Permian of the Paraná Basin. The CIA (molar) for the studied rocks accorded with expectations based on sedimentologic and paleontologic evidence, discriminating well between arid and humid conditions in the basin.

Acknowledgements

CNPq (Brazilian Research Council, Grant # 200453/97-1) is acknowledged for the doctorate scholarship granted to K. Goldberg, and UNISINOS for the logistics during field work and for the making of thin sections. Brazil's Department of Mining and Energy (DNPM/MME) and the Brazilian Geological Survey (CPRM) are thanked for access to cores and samples. We are in debt with Dr. David Archer for the access to the Atomic Absorption Spectrometer, and with Christine Braban for the careful instructions on the operation of the equipment. The manuscript greatly benefited from the corrections and suggestions of two reviewers and editor Finn Surlyk.

References

- Akarish, A.M., El-Gohary, A.M., 2008. Petrography and geochemistry of Lower Paleozoic sandstones, East Sinai, Egypt: Implications for provenance and tectonic setting. *Journal of African Earth Sciences* 52, 43–54.
- Alvarez, N.O.C., Roser, B.P., 2007. Geochemistry of black shales from the Lower Cretaceous Paja Formation, Eastern Cordillera, Colombia: Source weathering, provenance, and tectonic setting. *Journal of South American Earth Sciences* 23, 271–289.
- Bauluz, B., Mayayo, M.J., Fernandez-Nieto, C., Lopez, J.M.G., 2000. Geochemistry of Precambrian and Paleozoic siliciclastic rocks from the Iberian Range (NE Spain): implications for source-area weathering, sorting, provenance, and tectonic setting. *Chemical Geology* 168, 135–150.
- Diekmann, B., Wopfner, H., 1996. Petrographic and diagenetic signatures of climatic change in peri- and postglacial Karoo Sediments of SW Tanzania. *Palaeogeography, Palaeoclimatology, Palaeoecology* 125, 5–25.
- Driese, S.G., Nordt, L.C., Lynn, W.C., Stiles, C.A., Mora, C.I., Wilding, L.P., 2005. Distinguishing climate in the soil record using chemical trends in a vertisol climosequence from the

- Texas Coast Prairie, and application to interpreting Paleozoic paleosols in the Appalachian Basin, U.S.A. *Journal of Sedimentary Research* 75 (3), 339–349.
- Fairchild, T.R., Coimbra, A.M., Boggiani, P.C., 1985. Ocorrência de estromatólitos silicificados na Formação Irati (Permiano) na borda setentrional da Bacia do Paraná (MT, GO). *Anais da Academia Brasileira de Ciências* 57 (1), 117.
- Fedo, C.M., Young, G.M., Nesbitt, H.W., 1995. Unraveling the effects of potassium metasomatism in sedimentary rocks and paleosols, with implications for paleoweathering conditions and provenance. *Geology* 23 (10), 921–924.
- Gallala, W., Gaied, M.E., Montacer, M., 2009. Detrital mode, mineralogy and geochemistry of the Sidi Aich Formation (Early Cretaceous) in central and southwestern Tunisia: Implications for provenance, tectonic setting and paleoenvironment. *Journal of African Earth Sciences* 53, 159–170.
- Goldberg, K., 2001. The Paleoclimatic Evolution of the Permian of the Paraná Basin in southern Brazil. Ph.D. Dissertation, Department of Geophysical Sciences, University of Chicago, 267 pp.
- Gravenor, C.P., Rocha-Campos, A.C., 1983. Patterns of Late Paleozoic glacial sedimentation on the southeast side of the Paraná Basin, Brazil. *Palaeogeography, Palaeoclimatology, Palaeoecology* 43, 1–39.
- Gu, X.X., Liu, J.M., Zheng, M.H., Tang, J.X., Qi, L., 2002. Provenance and tectonic setting of the Proterozoic turbidites in Hunan, South China: Geochemical evidence. *Journal of Sedimentary Research* 72 (3), 393–407.
- Guerra-Sommer, M., Cazzulo-Klepzig, M., 2000. Early Permian palaeofloras from southern Brazilian Gondwana: a palaeoclimatic approach. *Revista Brasileira de Geociências* 30 (3), 482–486.
- Hamer, J.M.M., Sheldon, N.D., Nichols, G.J., 2007a. Global aridity during the Early Miocene? A terrestrial paleoclimate record from the Ebro Basin, Spain. *Journal of Geology* 115, 601–608.
- Hamer, J.M.M., Sheldon, N.D., Nichols, G.J., Collinson, M.E., 2007b. Late Oligocene–Early Miocene paleosols of distal fluvial systems, Ebro Basin, Spain. *Palaeogeography, Palaeoclimatology, Palaeoecology* 247, 220–235.
- Kasanzu, C., Maboko, M.A.H., Many, S., 2008. Geochemistry of fine-grained clastic sedimentary rocks of the Neoproterozoic Ikorongo Group, NE Tanzania: implications for provenance and source rock weathering. *Precambrian Research* 164, 201–213.
- Lavina, E.L., Faccini, U.F., 1993. Formações Pirambóia e Sanga do Cabral: um episódio de desertificação da Bacia do Paraná ao final do Permiano? 1 Simpósio sobre Cronoestratigrafia da Bacia do Paraná, Rio Claro, UNESP, pp. 94–95.
- Maynard, J.B., 1992. Chemistry of modern soils as a guide to interpreting Precambrian paleosols. *Journal of Geology* 100, 279–289.
- Melfi, A.J., Cerri, C.C., Kronberg, B.L., Fyfe, W.S., McKinnon, B., 1983. Granitic weathering: a Brazilian study. *Journal of Soil Science* 34, 841–851.
- Minyuk, P.S., Brigham-Grette, J., Melles, M., Borkhodoev, V.Ya., Glushkova, O.Yu., 2007. Inorganic geochemistry of El'gygytyn Lake sediments (northeastern Russia) as an indicator of paleoclimatic change for the last 250 kyr. *Journal of Paleolimnology* 37, 123–133.
- Nesbitt, H.W., Young, G.M., 1982. Early Proterozoic climates and plate motions inferred from major element chemistry of lutites. *Nature* 299, 715–717.
- Nesbitt, H.W., Young, G.M., 1984. Prediction of some weathering trends of plutonic and volcanic rocks based on thermodynamic and kinetic considerations. *Geochimica et Cosmochimica Acta* 48, 1523–1534.
- Nesbitt, H.W., Young, G.M., 1989. Formation and diagenesis of weathering profiles. *Journal of Geology* 97 (2), 129–147.
- Nowatzki, C.H., Dutra, T.L., Klein, C., 1996. Impressões de vegetais em depósitos de interdunas da Formação Sanga do Cabral (Permiano Superior–Triássico Inferior), RS. *Acta Geologica Leopoldensia* 19 (43), 25–42.
- Perez-Huerta, A.S., Sheldon, N.D., 2006. Pennsylvanian sea level cycles, nutrient availability and brachiopod paleoecology. *Palaeogeography, Palaeoclimatology, Palaeoecology* 230, 264–279.
- Price, J.R., Velbel, M.A., 2003. Chemical weathering indices applied to weathering profiles developed on heterogeneous felsic metamorphic parent rocks. *Chemical Geology* 202, 397–416.
- Rahman, M.J.J., Suzuki, S., 2007. Geochemistry of sandstones from the Miocene Surma Group, Bengal Basin, Bangladesh: implications for Provenance, tectonic setting and weathering. *Geochemical Journal* 41, 415–428.
- Rashid, S.A., 2005. The geochemistry of Mesoproterozoic clastic sedimentary rocks from the Rautgara Formation, Kumaun Lesser Himalaya: implications for provenance, mineralogical control and weathering. *Current Science* 88 (11), 1832–1836.
- Retallack, G.J., 1997. A colour guide to paleosols. Wiley, Chichester. 175 pp.
- Retallack, G.J., 2001. *Soils of the past*. Blackwell, Oxford. 600 pp.
- Retallack, G.J., 2005. Permian Greenhouse Crises. In: Lucas, S.G., Zeigler, K.E. (Eds.), *The Nonmarine Permian*, New Mexico Museum of Natural History and Science Bulletin, 30, pp. 256–269.
- Retallack, G.J., 2009. Greenhouse crises of the past 300 million years. *Geological Society of America Bulletin* 121, 1441–1455.
- Rohn, R., Fairchild, T.R., 1985. Estromatólitos permianos em calcário coquinóide do Grupo Passa Dois, nordeste do Paraná. *Anais da Academia Brasileira de Ciências* 57 (1), 118–119.
- Santos, P.R., Rocha-Campos, A.C., Canuto, J.R., 1996. Patterns of late Paleozoic deglaciation in the Paraná, Brazil. *Palaeogeography, Palaeoclimatology, Palaeoecology* 125, 165–184.
- Santos, R.V., Souza, P.A., Alvarenga, C.J.S., Dantas, E.L., Pimentel, M.M., Oliveira, C.G., Araújo, L.M., 2006. Shrimp U–Pb zircon dating and palynology of bentonitic layers from the Permian Irati Formation, Paraná Basin, Brazil. *Gondwana Research* 9, 456–463.
- Sayyed, M.R.G., Hundekari, S.M., 2006. Preliminary comparison of ancient bole beds and modern soils developed upon the Deccan volcanic basalts around Pune (India): potential for palaeoenvironmental reconstruction. *Quaternary International* 156–157, 189–199.
- Scheffler, K., Hoernes, S., Schwark, L., 2003. Global changes during Carboniferous–Permian glaciation of Gondwana: linking polar and equatorial climate evolution by geochemical proxies. *Geology* 31 (7), 605–608.
- Scheffler, K., Buehmann, D., Schwark, L., 2006. Analysis of late Paleozoic glacial to postglacial sedimentary successions in South Africa by geochemical proxies – response to climate evolution and sedimentary environment. *Palaeogeography, Palaeoclimatology, Palaeoecology* 240, 184–203.
- Sheldon, N.D., 2003. Pedogenesis and geochemical alteration of the Picture Gorge subgroup, Columbia River basalt, Oregon. *Geological Society of America Bulletin* 115 (11), 1377–1387.
- Sheldon, N.D., 2005. Do red beds indicate paleoclimatic conditions?: a Permian case study. *Palaeogeography, Palaeoclimatology, Palaeoecology* 228, 305–319.
- Sheldon, N.D., 2006. Abrupt chemical weathering increase across the Permian–Triassic boundary. *Palaeogeography, Palaeoclimatology, Palaeoecology* 231, 315–321.
- Sheldon, N.D., Tabor, N.J., 2009. Quantitative paleoenvironmental and paleoclimatic reconstruction using paleosols. *Earth Science Reviews* 95, 1–52.
- Sheldon, N.D., Retallack, G.J., Tanaka, S., 2002. Geochemical Climofunctions from North American Soils and Application to Paleosols across the Eocene–Oligocene Boundary in Oregon. *Journal of Geology* 110, 687–696.
- Singh, B.P., Tandon, S.K., Singh, G.P., Pawar, J.S., 2009. Paleosols in early Himalayan foreland basin sequences demonstrate latitudinal shift-related long-term climatic change. *Sedimentology* 56 (5), 1464–1487.
- Sinha, S., Islam, R., Ghosh, S.K., Kumar, R., Sangode, S.J., 2007. Geochemistry of Neogene Siwalik mudstones along Punjab re-entrant, India: implications for source-area weathering, provenance and tectonic setting. *Current Science* 92 (8), 1103–1113.
- Soreghan, M.J., Soreghan, G.S., 2007. Whole-rock geochemistry of upper Paleozoic loessite, western Pangaea: implications for paleo-atmospheric circulation. *Earth and Planetary Science Letters* 255, 117–132.
- Spalletti, L.A., Queralt, I., Matheos, S.D., Colombo, F., Maggi, J., 2008. Sedimentary petrology and geochemistry of siliciclastic rocks from the upper Jurassic Tordillo Formation (Neuquén Basin, western Argentina): implications for provenance and tectonic setting. *Journal of South American Earth Sciences* 25, 440–463.
- Visser, J.N.J., Young, G.M., 1990. Major element geochemistry and paleoclimatology of the Permo–Carboniferous glaciogene Dwyka Formation and post-glacial mudrocks in southern Africa. *Palaeogeography, Palaeoclimatology, Palaeoecology* 81, 49–57.
- Xiao, S., Liu, W., Li, A., Yang, S., Lai, Z., 2010. Pervasive autocorrelation of the chemical index of alteration in sedimentary profiles and its palaeoenvironmental implications. *Sedimentology* 57, 670–676.
- Young, G.M., 2002. Stratigraphic and tectonic settings of Proterozoic glaciogenic rocks and banded iron-formations: relevance to the snowball Earth debate. *Journal of African Earth Sciences* 35, 451–466.
- Young, G.M., Nesbitt, H.W., 1999. Paleoclimatology and provenance of the glaciogenic Gowganda Formation (Paleoproterozoic), Ontario, Canada: a chemostratigraphic approach. *GSA Bulletin* 111 (2), 264–274.
- Young, G.M., von Brunn, V., Gold, D.J.C., Minter, W.E.L., 1998. Earth's oldest reported glaciation: physical and chemical evidence from the Archean Mozaan Group (2.9 Ga) of South Africa. *Journal of Geology* 106, 523–538.
- Zaghoul, M.N., Critelli, S., Perri, F., Mongelli, G., Perrone, V., Sonnino, M., Tucker, M., Aiello, M., Ventimiglia, C., 2010. Depositional systems, composition and geochemistry of Triassic rifted-continental margin redbeds of the Internal Rif Chain, Morocco. *Sedimentology* 57, 312–350.
- Zálan, P.V., Wolff, S., Conceição, J.C.J., Astolfi, M.A.M., Vieira, I.S., Appi, V.T., Zanotto, O.A., Marques, A., 1991. Tectonics and sedimentation of the Paraná Basin. In: Ulbrich, H., Rocha-Campos, A.C. (Eds.), *Proceedings of the 7th International Gondwana Symposium*. São Paulo, Instituto de Geociências, USP, pp. 83–117.
- Zech, M., Zech, R., Zech, W., Glaser, B., Brodowski, S., Amelung, W., 2008. Characterisation and palaeoclimate of a loess-like permafrost palaeosol sequence in NE Siberia. *Geoderma* 143, 281–295.
- Ziegler, A.M., Hulver, M.L., Rowley, D.B., 1997. Permian world topography and climate. In: Martini, I.P. (Ed.), *Late glacial and postglacial environmental changes*. Oxford University Press, pp. 111–146.
- Zimmerman, U., Bahlburg, H., 2003. Provenance analysis and tectonic setting of the Ordovician clastic deposits in the southern Puna Basin, NW Argentina. *Sedimentology* 50, 1079–1104.